

Steady State Analyse of existing Compressed Air Energy Storage Plants

Thermodynamic Cycle modeled with Engineering Equation Solver

Friederike Kaiser

Energie-Forschungszentrum Niedersachsen (EFZN)
 Goslar, Germany
 f.kaiser@efzn.de

Abstract—As compressed air energy storage (CAES) is a promising energy storage technology that has already proven its reliability in commercial operation some basic thermodynamic information on this process are elaborated in this paper. It shows a comparison of the thermodynamic process cycles of the CAES plants in Huntorf and McIntosh that has been modeled in EES (Engineering Equation Solver). Detailed T-s-Diagrams are given to show the differences of reversible and irreversible thermodynamic modeling of CAES. It is demonstrated that irreversibility assumption leads to an over estimation of the plant efficiency and therefore newer CAES concepts (like adiabatic CAES) should not be approximated with reversibility assumptions to avoid misleading statements.

Keywords - CAES; energy storage; EES; thermodynamic cycle comparison, renewable energy, Energiewende

I. ENERGY STORAGE FOR RENWEABLES

The switch from fossil energy sources to energy generation with renewable sources like wind power and photovoltaic leads to a mismatch of power supply and demand. Nevertheless the German government pursues the so called ‘Energiewende’. The installation of additional renewable energy plants is highly encouraged and financially supported. Two of the main pillars of renewable energy are wind and solar power. These two vary within the time of day and season disregarding the power demand and furthermore causing high power gradients that can destabilize the grid. The temporal mismatch of supply and demand as well as the high power gradients can be suspended by the use of energy storage technologies that supply regulating energy.

In the field of large commercial mechanical energy storage pumped hydro energy storage (PHES) and compressed air energy storage (CAES) are suitable technologies to deliver flexible power within a wide regulation range and to store energy for intermediate term with little storage losses. Both technologies PHES and CAES have proven their feasibility and reliability in commercial use for several decades. While installed power of PHES exceeds seven Gigawatts in Germany alone, the installed power of CAES plants is limited to only 432 MW worldwide. The two existing commercial plants

Huntorf and McIntosh are analyzed in detail in this paper from a thermodynamic point of view.

II. GENERAL DESCRIPTION OF CAES

The CAES process is similar to the gas turbine or Joule process (also called Brayton process) with the addition of a temporary storage of compressed air after the compression [1]. This automatically leads to a decoupling of compressor and expander, which are usually complementary parts of the same drive shaft. A conventional gas turbine consists of one shaft with compressor, combustion and expander zone as parts of the same rotating equipment.

The following simplified process flow (a and b) and T-s-diagrams (c and d) show the conventional open Joule/ Brayton cycle (a and c) in comparison with CAES cycle (b and d):

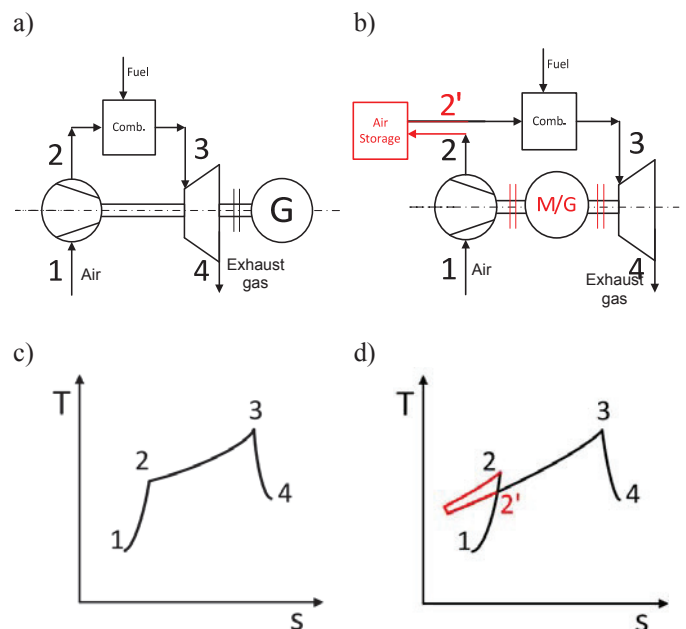


Figure 1. Schematic process flow and T-s-diagram of the Joule and CAES-Process to show the similarities and difference between both processes.

The process is simplified to 4 state points with 1-2 air compression (1-2' compression and air storage), 2(2')-3 combustion and 3-4 expansion. Figure 1 shows that the actual storage (from 2-2') is an anti clockwise process in the T-s-diagram which means energy is being consumed.

A. Huntorf

The first CAES plant worldwide has been commissioned in 1978 in Huntorf, Germany. Today it has a turbine output power of 321 MW with a discharge time at full load of 2 hours. The charging time is with 6 hours three times higher as the compressor train runs only 60 MW.

Huntorf uses two solution-mined salt caverns for air storage. There is no heat cycling: neither heat storage of the compression heat nor heat recovery of the exhaust gas. Due to this Huntorf can be regarded as the basic plant configuration. Nevertheless – as first of its kind – it included some unprecedented technologies like a high pressured combustion and ignition or special couplings for high driving speed and high power [2]. Its original purpose is the back up of other regional power plants especially due to its ability for black start [2].

Some process design parameters of temperature and pressure from the Huntorf steady state cycle are known from [2] and [3]. The following table gives an overview of these process parameters that serve as input values for the calculation of the unknown process parameters.

TABLE I. PROCESS PARAMETER OF HUNTORF CAES [2][3]

| State point | Process Conditions | | |
|-------------|--|-----------------|---------------------|
| | Process Point Description | pressure in bar | temperature |
| 1 | ambient conditions | 1,013 | 281 K ^{a)} |
| 2 | outlet 1 st compression stage | 6 | |
| 4 | outlet 2 nd compression stage | 46-72 | |
| 5 | after cooler exit/cavern inlet | | 322 K |
| 7 | throttle outlet | 46 | |
| 8 | inlet 1 st expansion stage | 41,3 | 763 K |
| 10 | inlet 2 nd expansion stage | 12,8 | 1218 K |
| 11 | outlet 2 nd expansion stage | 1,1 | |

a) .average temperature at Huntorf site

B. McIntosh

The McIntosh plant had its start up in 1991 in Alabama, U.S. The power output of 110 MW is lower than Huntorf's, but the energy content or capacity (which is determined by the air storage size) is with 26 hours at maximal load more than four times higher.

The major advantage of McIntosh's plant configuration over Huntorf is the addition of exhaust heat recuperation. The stored air is preheated before the combustion with the help of the hot exhaust gas, which leads to an augmentation of process

efficiency as will be shown in detail hereinafter. Furthermore a 4-stage compression has been chosen in contrast to Huntorf, with two stages only.

The following table gives the process parameter of McIntosh's CEAS plant.

TABLE II. PROCESS PARAMETER OF MCINTOSH CAES [3][4]

| State point | Process Conditions | | |
|-------------|--|-----------------|---------------------|
| | Process Point Description | pressure in bar | temperature |
| 1 | ambient conditions | 1,013 | 281 K ^{a)} |
| 2 | outlet 1 st compression stage | 4.1 | |
| 4 | outlet 2 nd compression stage | 10.3 | |
| 6 | outlet 3 rd compression stage | 26.9 | |
| 8 | outlet 4 th compression stage | 62-80 | |
| 9 | after cooler exit/cavern inlet | | 316,5 K |
| 11 | throttle outlet | 50,7 | |
| 12 | exhaust heat recuperator exit | | 568 K |
| 13 | inlet 1 st expansion stage | 43 | 810 K |
| 15 | inlet 2 nd expansion stage | 15 | 1144 K |
| 16 | outlet 2 nd expansion stage | 1,04 | |

a) .average temperature at Huntorf site

III. PROCESS UNITS OF CAES

In order to built up a model for the calculation of the thermodynamic cycle of CAES the basic process units have to be clarified. The process units compression, air and heat storage, throttling, expansion as well as heat exchange and combustion (described hereinafter in detail) are modeled within the program EES – Engineering Equation Solver. This program contains a wide data base of different fluid properties and equations of state. With two state properties a third can easily be calculated by its corresponding function. Besides state properties any other calculation has to be noted as equation (rather than assignments) and is solved by EES numerically.

A. Compression

During compression the working fluid is compressed from an initial pressure p_i to an outlet pressure p_o . Temperature is rising from T_i to T_o , where T_o is unknown and has to be calculated. For an ideal gas this can be done with the equation:

$$T_{o,rev.} = T_i \cdot (p_o/p_i)^{\kappa-1/\kappa}, \quad (1)$$

which can be derived from first law of thermodynamic for closed static systems (no potential, no kinetic energy) where any change of the inner energy equals changes of work and heat:

$$dU = \delta W + \delta Q. \quad (2)$$

For an adiabatic process with $\delta Q = 0$ and ideal gas assumption $dU = c_v \cdot dT$ and reversibility assumption $\delta W = -p \cdot dv$ we get the equation

$$c_v dT = -p dv. \quad (3)$$

In combination with the ideal gas law $p = R \cdot T/v$ and after integration within the limits T_i to T_o and v_i to v_o the following statement appears:

$$c_v \ln(T_o/T_i) = -R/c_v \ln(v_o/v_i) = \ln(v_o/v_i) - R/c_v. \quad (4)$$

For an ideal gas it can be assumed that $c_p = c_v + R$ and the ideal gas law helps to replace v with p to get equation (1), where $\kappa = c_p/c_v = 1.4$ for air as ideal gas.

The assumption that air behaves like an ideal gas is only in a pressure range close to atmospheric pressure suitable and is not sufficiently accurate for the entire CAES process (usually going up to 70 bars or higher). Therefore the actual CAES model is programmed in EES (Engineering Equation Solver) which uses more accurate equations of state, namely the calculations based on Lemmon et al. "Thermodynamic Properties of Air and Mixtures of Nitrogen, Argon, and Oxygen From 60 to 2000 K at Pressures to 2000 MPa" [5]. The programming code to obtain a state variable is limited to a simple statement, e.g. to get the entropy: "si = entropy('Air_ha', p=p_i, T=T_i)", where "entropy(...)" is an EES function name that reflects in combination with the fluid name "Air_ha" the equations according to [5] – an equation of state for dry air.

The corresponding manual calculation (e.g. for verification of EES' results) can be done by looking up the property table [5] with $s_i(T_i, p_i)$ or can be calculated with the actual equation of state shown in [5] that is:

$$Z = p/\rho RT = 1 + \delta(d\alpha^f/d\delta)_T, \quad (5)$$

with α^f as the residual Helmholtz energy as a function of the (reduced) pressure and temperature and 76 constants. Further equations for the calculation of state variables are given in [5] as well as the estimated uncertainty of the results that are generally accurate to within 1 %.

Besides the equation of state, the primarily met reversibility assumption is not realistic. In a real irreversible process energy is dissipated and the isentropic efficiency η_s has to be considered when calculation the technical work

$$w = w_{\text{reversible}}/\eta_s. \quad (6)$$

This affects the temperature after compression as follows:

$$T_o = T_i + (T_{o,\text{rev}} - T_i) / \eta_s, \quad (7)$$

when assuming that the variation of $c_{p,i}(T_i)$ is small and a medium $c_{p,m}$ can be used for the temperature range T_i to T_o). A realistic value for the isentropic efficiency of a compressor lies in the range $0.7 < \eta_s < 0.88$ [6]. In the model at hand an isentropic efficiency for the compression of $\eta_s < 0.80$ is chosen.

B. Air and Heat storage

There are many possible pressure containers: solution mined salt caverns, mined hard rock caverns, porous rock such as aquifer [7] or depleted gas field [8], [9] as well as vessels for smaller applications and pressure bags for off shore applications. More costly and therefore less probable

alternatives are pipe batteries, cryogenic storage, absorption and adsorption in solids and liquids and reversible chemical combinations. [10] All of these options lead to the major challenge of CAES: the pressurized stored air should not exceed a certain temperature limit in order to assure storage integrity. Therefore a large amount of heat has to be removed from the compressed air stream before storage and either being dissipated or stored for the later use in the expansion process which leads over to the theoretical concept of "adiabatic CAES" (A-CAES), where no heat other than the compression heat is used to run the turbine process. In this concept no heat in form of fuel combustion is added to the process.

Heat can be stored in different ways: as sensible heat of a gas, liquid or solid as well as latent heat of a phase change, e.g. water vaporization and condensation.

The relevant temperature range for the heat storage in CAES concepts reaches from ambient to the maximum compression temperature. In the case of adiabatic concepts this can -in theory- be more than 900 K [11] or in a practical example for Huntorf 614 K. A realistic limit for available turbo compressors is up to 675 K [4].

The heat transfer medium has to be chosen according to the temperature level of the specific process. In the case of ADELE, an adiabatic CAES concept, for example sensible heat storage in fireproofed stoneware has been researched for a temperature level above 973 K [11].

C. Throttle

Another major issue linked to the air storage is the pressure inside the storage reservoir. Cavities, caverns and vessels are isochoric tanks. During expansion the storage tank is being discharged and pressure drops, meanwhile the input pressure for the expander is required to vary only in a minimal range to make sure high efficiency during expansion. To bring together both requirements air can be stored in the tank with a surplus pressure and being throttled down to the required expander input pressure. This is obviously linked to efficiency loss. The implementation of an isobaric pressure tank is promising, but causes higher technical effort in the realization. There are several concepts addressing the isobaric storage option such as "ISACOST-CC" [3] or the off shore pressure bags [12].

The throttling process is modeled according to the Joule-Thomson-Effect assuming an isenthalpic pressure change. To calculate the resulting temperature the Joule-Thomson coefficient μ_{JT} has to be determined from the Van-der-Waals-coefficients a_L , b_L and fluid property molar heat capacity c_{pm} through: $\mu_{JT} = ((2a_L/(R \cdot T_i)) - b_L) / c_{pm}$. The temperature drop of the throttle can then be calculated with:

$$\Delta T = (p_i - p_o) \cdot \mu_{J,T} \quad (8)$$

D. Expansion

Analogue to the compression, expansion outlet temperature T_o can be approximated based on the assumptions of ideal gas and reversibility which gives the outlet temperature (reversible)

$$T_{o,\text{rev.}} = T_i \cdot (p_o/p_i)^{\kappa-1/\kappa}. \quad (9)$$

Considering the isentropic efficiency (irreversibility) of the turbine that lies between $0,7 < \eta_s < 0,88$ [6], the actual outlet temperature of the expansion is (for ideal gas)

$$T_o = T_i - \eta_s (T_i - T_{o,rev}). \quad (10)$$

The EES model uses the more precise equation of state for air according to [5]. In the model at hand an isentropic efficiency for the expansion of $\eta_s < 0.80$ is chosen.

E. Heat exchange and combustion

Thermal cycling of compression heat and exhaust heat recuperation strongly influence the process efficiency. During compression a relatively high temperature level is reached that could exceed the capability of the compressor and of the following air storage. Due to this, compression in many CAES concepts is subdivided in several stages, intermitted by inter cooling (in Huntorf with cooling water [2]) and followed by an after cooler. The negative side effect of these heat exchangers is the pressure drop. To include this loss into the EES program a basic tubular heat exchanger is modeled using the following assumptions: cross flow, two inner and one outer passes, compressed air on tube side, cooling water on shell side, sufficient number of deflectors, fixed tube diameter, wall thickness and roughness. For any input of working fluid temperatures and pressures (inlet and outlet) as well as mass flow and maximum flow rate a dimensioning of basic tubular heat exchanger is accomplished and its resulting pressure drop is calculated on the basis of [13] Chapters A2, B2, C1, C3, G1.

IV. RESULTING T-S-DIAGRAMMS

From the above mentioned equations and under consideration of the plant configuration and design parameters of Huntorf and McIntosh the following T-s-Diagrams results:

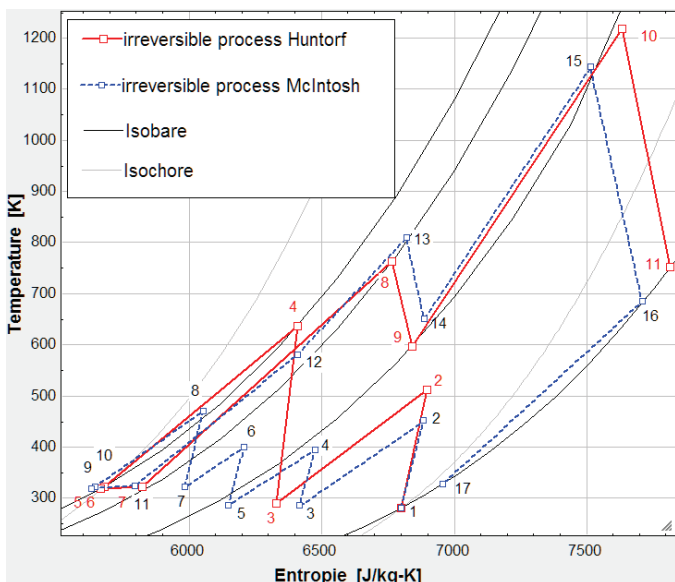


Figure 2. T-s-Diagram of Huntorf and McIntosh CAES processes

Several differences between Huntorf and McIntosh can be seen in Figure 2: Huntorf has 2 compression stages (1-2, 3-4), McIntosh has 4 compression stages (1-2, 3-4, 5-6, 7-8). That

automatically implies a lower temperature level in McIntosh's compressor train: lower than 500 K compared to Huntorf's over 600 K. The storage and expansion of both plants is quite similar. One major difference consists in the exhaust heat recuperation: McIntosh state point 11-12 is the air preheating with exhaust heat from 16-17. Huntorf entirely heats the air through natural gas combustion. The exhaust temperature of Huntorf is over 700 K while McIntosh's exhaust gas is close to ambient conditions.

The overall process efficiencies of both plants differs of about 12 percent points. Typically in literature Huntorf is cited with 42 % and McIntosh with 54 %. These values probably apply to the optimal operation conditions when no throttling is necessary. The calculation showed that the efficiency drops of about 2 to 3 % when maximal throttling (in the case that maximal charging level of the storage cavern is reached) is considered: Huntorf 40.4 % and McIntosh 51.1 %.

To demonstrate the necessity of irreversible calculation the following figure shows the Huntorf process under reversibility assumption.

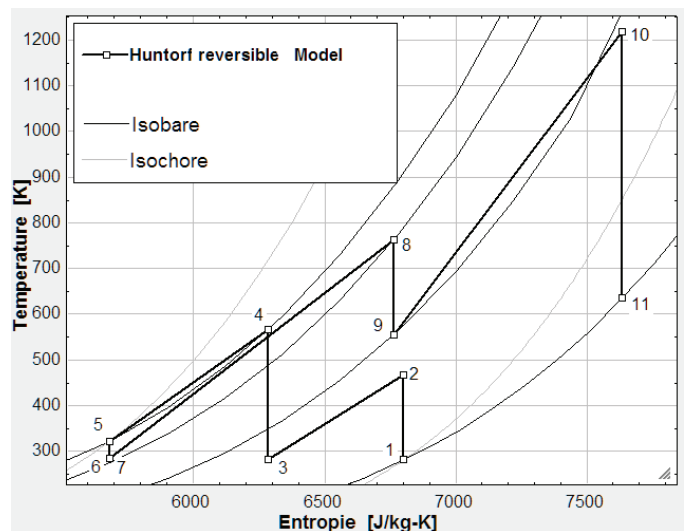


Figure 3. T-s-Diagram of Huntorf under reversibility assumptions

When idealizing Huntorf to a reversible process the maximal compression temperature (state point 4) is less than 600 K. Furthermore the efficiency of the overall plant rises to over 54 % which is 10 % over the actual plant efficiency. Accordingly any CAES calculation using reversibility assumption can only have a limited validity.

V. DISCUSSION

The model programmed in EES gives accurate results for the plant configurations Huntorf and McIntosh. Plant efficiencies correspond to the well known literature values. The resulting T-s-diagrams can be considered to give a good impression of the process cycles and operation parameters. But it has to be taken into account, that only the state points have been subject of the calculation, the connecting graphs are simplified to straight lines whereas curved trajectories would be more precise (e.g. in Fig. 2 the trajectory for the change of

state 16-17 would have to follow the corresponding isobaric graph).

The impact of changing ambient temperature is considerable and has not been subject of the analysis in this paper.

All calculations have been executed with the equations of state according to [5] for dry air. As the air at compression inlet corresponds to ambient conditions and as the air is stored in both plant configurations Huntorf and McIntosh in salt caverns that contain a certain amount of water it would be more precise to use property data of humid air. Any condensation and vaporization and its impact on the temperature has not been taken into account. Reference [4] showed that the effect of air humidity should not be neglected. Further improvements to the model at hand should be made especially concerning humidity.

An isentropic efficiency of 0.8 has been assumed for each compression and expansion stage. This value is within a realistic range, but the actual values may vary with approximately +/-0.1 which strongly influences the overall plant efficiency. The exact isentropic efficiencies of machinery at Huntorf and McIntosh plant are not published.

The heat loss during storage has not been taken into account because the air is cooled down approximately to the cavern temperature. Nevertheless could this model be improved by considering a possible temperature drop or rise depending on the storage condition.

ACKNOWLEDGMENT

Thanks to Prof. Roman Weber for his support as well as to the Energy Research Center Lower-Saxony for the opportunity of working in the field of energy storage.

REFERENCES

- [1] Giramont, Albert J.; Lessard, Robert D.: Exploratory Evaluation of Compressed Air Storage Peak-Power Systems (1974). in Energy Sources, Vol. 1, No. 3, Connecticut 1974
- [2] BBC AG (Hrsg.): Huntorf Air Storage Gas Turbine Power Plant (um 1980). in Sonderdruck Energy Supply Publication No. D GK 90 202 E, Mannheim
- [3] Nielsen, Lasse: GuD-Druckluftspeicherkraftwerk mit Wärmespeicher. Schriftenreihe des Energie-Forschungszentrums Niedersachsen EFZN, Band 14, Cuvillier Verlag Göttingen, 2013
- [4] Wolf, Daniel: Methods for design and application of adiabatic compressed air energy storage based on dynamic modeling. Dissertation, Laufen, Oberhausen. UMSICHT-Schriftenreihe Band 65, p.167, 2011 ISBN: 978-3-87468-264-0
- [5] Lemmon et al.: Thermodynamic Properties of Air and Mixtures of Nitrogen, Argon, and Oxygen From 60 to 2000 K at Pressures to 2000 MPa. J. Phys. Chem. Ref. Data, Vol. 29, No. 3, Pages 331-385, 2000
- [6] Borgnakke, Claus; Sonntag, Richard E.: Fundamentals of Thermodynamics. 7th Edition, John Wiley and Sons (Asia) Pte Ltd, 2009, ISBN 978-0-470-17157-8
- [7] Succar, Samir; Williams, Robert H.: Compressed Air Energy Storage: Theory, Resources, And Applications (2008). Energy Systems Analysis Group, Princeton Environmental Institute (PEI), 8 April 2008
- [8] EPRI-DOE Handbook of Energy Storage for Transmission and Distribution Applications, EPRI, Palo Alto, CA, and the U.S. Department of Energy, Washington, DC: 2003. 1001834.
- [9] Kushnir, Roy; Dayan, Abraham; Ullmann, Amos: Thermodynamic and hydrodynamic response of compressed air energy storage reservoirs: a review (2012). in Rev Chem Eng 28 (2012) S.123–148, Berlin DOI 10.1515/revce-2012-0006
- [10] National Research Council (U.S.): Assessment of Technology for Advanced Power Cycles. Ad Hoc Panel on Advanced Power Cycles. National Academy of Science, Washington 1977
- [11] RWE: ADELE – Der adiabate Druckluftspeicher für die Elektrizitätsversorgung. RWE Power AG Sonderdruck 2010 www.rwe.com/rwepower
- [12] Pimm; Garvey; Drew: Shape and cost analysis of pressurized fabric structures for subsea compressed air energy storage (2014). in Proceedings IMechE Vol. 225 Part C: Journal of Mechanical Engineering Science, Nottingham, 2014
- [13] VDI-Wärmeatlas. 11., bearbeitete und erweiterte Auflage. Verein Deutscher Ingenieure VDI-Gesellschaft Verfahrenstechnik und Chemieingenieurwesen (GVC), Düsseldorf, Springer Heidelberg 2012, ISBN 978-3-642-19980-6, DOI 10.1007/978-3-642-19981-3